



SOOTY FRUIT: Fruits Item Classification Using Sooty Tern Optimized Deep Learning Network

Josephin Shermila. P^{1*}Seethalakshmi. V¹Ahilan. A²Devaki. M³

¹*Department of Artificial Intelligence and Data Science,
R.M.K. College of Engineering and Technology, Chennai, Tamilnadu, India*

²*Department of Electronics and Communication Engineering,
PSN college of engineering and technology, Tirunelveli, Tamilnadu, India*

³*Department of Electronics and Electrical Engineering,
Velammal College of Engineering and Technology, Madurai, Tamilnadu, India*

* Corresponding author's Email: josephinshermila21pp@outlook.com

Abstract: Fruits are structures that contain seeds that are created from the ovaries of only blooming plants. A fruit is a soft, component of a blooming plant that bears seeds. It is created from angiosperm ovaries and is unique to this plant group. In this paper proposed a novel Deep Learning-based Fruits Items Classification (SOOTY FRUIT) method to classify the variety of Fruits items from the dataset with their calorie values (CV). Initially, the images are processed using the Gaussian adaptive bilateral (GAB) Filter approach to improve image quality and eliminate noise. Consequently, the segmented images are pre-processed utilizing Attention V-net algorithm. The extracted features are then normalized utilized the Sooty Tern Optimization Algorithm (STOA). Fruits items are classified using Ghostnet based on these relevant features. As compared to existing methods, the proposed SOOTY FRUIT shows better results in terms of Accuracy. The accuracy of the proposed technique can be as high as 99.95%, while that of traditional models like the attention-based densely connected convolutional networks with convolution autoencoder (CAE-AND), Faster-Region-based Convolutional Neural Network (F-RCNN), and Attention Fusion Network (AFN) is 84.9%, 87.58%, and 93.91%, respectively.

Keywords: Deep learning, Gaussian adaptive bilateral filter, Ghostnet, Sooty tern optimization algorithm.

1. Introduction

Abnormal or excessive fat buildup that poses a health concern is what is meant to be understood as being overweight or obese. Over 25 is deemed overweight, and over 30 is obese based on body mass index (BMI) [1, 2]. The worldwide burden of illness report from 2017 states that the problem has reached epidemic proportions, with over 4 million deaths annually attributable to overweight or obesity [3, 4].

One aspect of the double burden of malnutrition is obesity, and everywhere except sub-Saharan Africa and Asia, more people are fat than underweight today [5]. Overweight and obesity, which were previously thought to be issues exclusive to high-income nations, are now sharply increasing in low- and middle-

income nations, especially in metropolitan areas [6, 7]. The majority of children who are overweight or obese reside in developing nations, where the pace of rise in comparison to industrialized nations has exceeded thirty percent [8].

The calorie is a unit of energy derived from the now-defunct caloric theory of heat. There are two primary meanings of "calorie" that are commonly used for historical reasons [9]. The big calorie, also known as the fruit calorie, dietary calorie, or kilogram calorie, was first described as the quantity of heat required to increase one kilogram of water's temperature by one degree Celsius (or one kelvin) [10, 11]. The definition of the tiny calorie, often known as the gram calorie, is the quantity of heat required to raise one gram of water by the same amount. One

large calorie is therefore equivalent to 1000 little calories.

Furthermore, contemporary techniques have a number of limitations, namely low accuracy, considerable fluctuation in calorie content, and inaccurate results obtained during calorie measurement leading to misclassification [12]. A novel deep learning-based Fruits classification technique (SOOTY FRUIT) was proposed to tackle this problem. It uses a dataset's CV to classify different meals. The work's primary contribution has been succeeded by

- Initially, the images are processed using the Gaussian adaptive bilateral Filter (GAB) approach to improve image quality and eliminate noise.
- Consequently, the segmented images are pre-processed utilizing Attention V-net algorithm.
- The extracted features are then normalized utilized the Sooty Tern Optimization Algorithm (STOA).
- Fruits items are classified using Ghostnet based on these relevant features.

The remaining portion of the work has been followed by, Section 1 illustrates the Introduction of the proposed and Section 2 illustrates the Literature Survey of the work, Section 3 illustrates the Proposed Methodology, Section 4 illustrates the Result and Discussion of the work and finally the section 5 illustrates the Conclusion of the proposed.

2. Literature review

In several studies, neural networks and traditional DL methods were utilized to Classify the Fruits items. This section will provide a brief summary of several tactics.

In 2020 Xue, G., et al., [13] developed a densely connected convolutional network with convolutional autoencoder (CAE-ADN) hybrid deep learning framework for classifying fruit images. The effectiveness of the technique is tested on two fruit datasets. Experimental results illustrate the utility of our methodology. This framework increases fruit sorting efficiency and decreases costs for fresh supply chains, manufacturers, supermarkets, and other organizations.

In 2019 Wasif et al., [14] recommended that a faster RCNN (F-RCNN) be used in order to find and get a cutting technique for feature extraction (FE) and segmentation. Then, using the probing item, determine the known volume and measure the volume of the meal. Volume is used to determine a

food's calorie amount, but this method can be challenging.

In 2022 Gill, H.S. and Khehra, B.S., et al., [15] suggested a Deep Learning application for classifying images of fruit. CNN is utilized to identify the optimal features. Features are labeled using RNN. Gradients that explode and vanish during RNN marking are handled by the LSTM algorithm. We conducted extensive experiments on fruit photographs using both the proposed method and existing competing technologies. Increasing the dataset from 40% to 50%, 50% to 60%, and 60% to 70% does not change the categorization rate during the procedure.

In 2023 Mahgoub, H., et al., [16] develops a Bio-Inspired Spotted Hyena Optimizer using the Deep Convolutional Neural Network-based Automated Food Image Classification (SHODCNN-FIC) technique. The main objective of the SHODCNN-FIC approach is to recognize and classify food photos into several groupings. The SHODCNN-FIC approach is shown here, which leverages the DL model for food photo classification using a hyperparameter tuning strategy. The Extreme Learning Machine (ELM) model is employed by the SHODCNN-FIC technique to detect and categorize food photos. Extensive experiments were conducted to demonstrate the superior performance of the proposed SHODCNN-FIC approach in food picture classification.

In 2023 Gulzar, Y., [17] developed the deep learning model TL-MobileNetV2. Data from a set of forty different fruits were used to train and evaluate the proposed model. After removing the categorization layer from the MobileNetV2 architecture, five more layers were added to the TL-MobileNetV2 model in order to improve the model's efficacy and accuracy. We also used a range of preprocessing and model tuning techniques to ensure that TL-MobileNetV2 performed well on the previously described datasets without overfitting. Experimental results show that TL-MobileNetV2 obtained 99% accuracy on the fruit dataset.

In 2019 Zhang, Y.D., et al., [18] developed a 13-layer deep convolutional neural network for fruit classification. Experimental results show that our CNN outperforms five state-of-the-art techniques with an overall accuracy of 94.94%. Through data augmentation, the training set of data is expanded from 1,800 to 63,000. The maximum pooling technique performs somewhat better than average pooling. We also validated the optimum CNN structure. The classifier lost around 5% of its overall accuracy when we tested it with incomplete photos. According to a time study, the GPU can speed test

data by 175x and training data by 177x. The extension of data was verified to be successful.

In 2020, Liu, C., et al., [19] suggested an Attention Fusion Network (AFN) and a Food-Ingredient Joint Learning module for fine-grained food and ingredient recognition. Based on studies on the fine-grained Chinese food dataset VIREO Food-172, the findings of ingredients recognition are state-of-the-art.

In 2022, Wang, Z., et al. [20] suggested a framework for ingredient-oriented multitasking that enables the simultaneous prediction of components and food recognition. Extensive experimental results on three popular datasets have demonstrated the effectiveness of the approach. The superiority of the strategy is further illustrated by further visualisations of attention maps and ingredient assignment maps. The main drawbacks of traditional methods are low accuracy, high variation in misclassification, and calorie content. To overcome this issue a novel DL-based Fruits classification (SOOTY FRUIT) has been proposed.

3. Proposed methodology

In this section, a novel DL-based Fruits items classification method (SOOTY FRUIT) was proposed to classify different Fruits from the dataset by CV. In the first, the sigmoid stretching methods the images are processed utilized to increase the image quality and remove the noises. Consequently, the segmented images are pre-processed utilizing U-

net algorithm. The extracted features are then normalized utilized the Sooty Tern Optimization Algorithm (STOA). Fruits items are classified using Ghostnet based on these relevant features. Fig. 1 illustrate the proposed methodology.

3.1 Dataset

We used the dataset from for this investigation. This dataset, which includes 20 different types of fruits and vegetables, was used in this study. The data is divided into 16 distinct categories, including 8 for fruits and 8 for vegetables. Each class receives a unique selection of five vegetables and fruits. However, some meals feature simply four types of fruits and vegetables. Fruits and vegetables were shot on plates of varying sizes, shapes, and colors. The collection has roughly 41,509 images, with approximately 4,000 images each class.

3.2 Pre-processing via GAB filter

Pre-processing is a process utilized to enhance the precise features and eliminate undesired noise from an input image. Herein Gaussian adaptive bilateral filter (GABF) is utilized to eliminate the noise. GABF is an edge-preserving, smoothing, noise-reducing Filter. The Bilateral filter diminishes significantly when the guidance (n) and noise input (i) are similar. The kernel range is corrupted with improver noise, so the bilateral kernel offers limited smoothing.

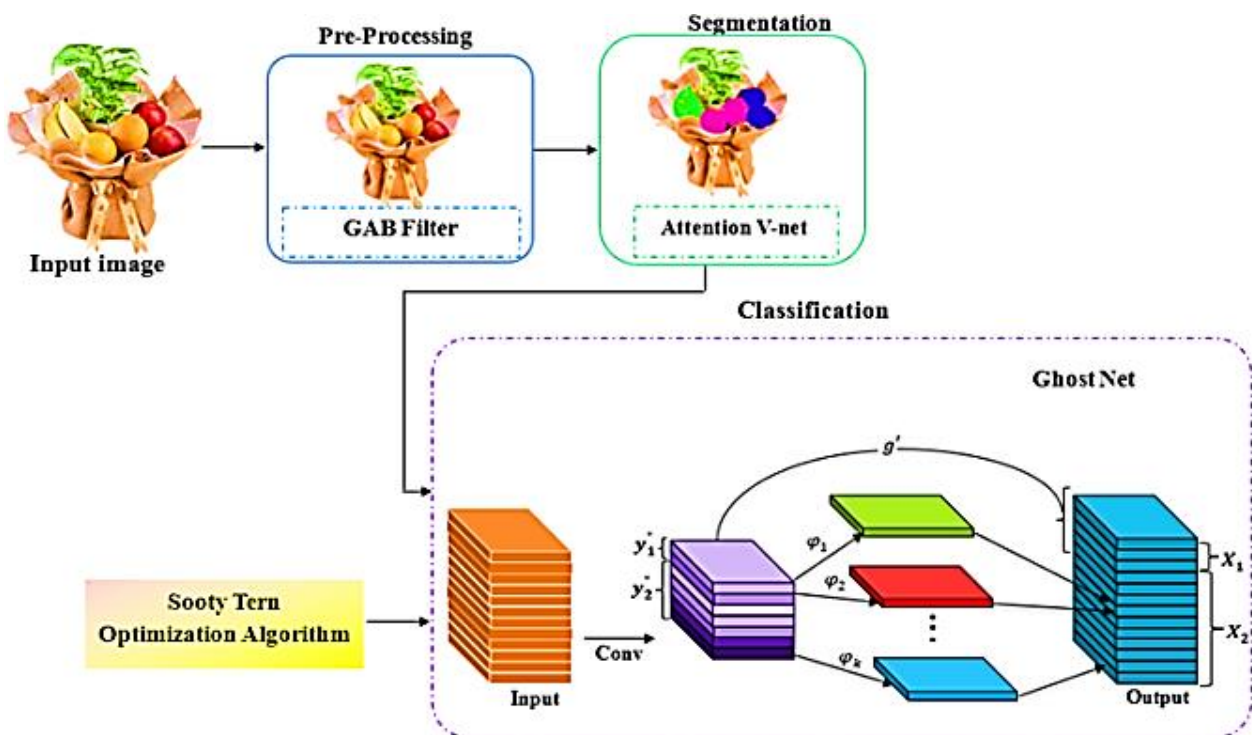


Figure. 1 Proposed Methodology

The GABF technique assumes that n and i are not identical, which implies that a low-pass filter is applied to guide the range kernel, and image contours are strictly preserved.

A low-pass guidance image is first produced for a given image i by applying the Gaussian blur process. The weighted average is calculated using pixels in adjacent positions with descending weights. The process can be explained as follows:

$$B(I) = \sum_m X_{pq}^n(n) i_m \quad (1)$$

The filter kernel can be computed as follows,

$$X_{p,q}^n(n) = \frac{1}{r_p} \exp \left[-\frac{\|p-q\|^2}{\sigma_j^2} \right] \quad (2)$$

The GABF can be computed as follows,

$$X_{p,q}^{nuvf}(i, \bar{n}) = \frac{1}{r_p} \exp \left[-\frac{\|p-q\|^2}{\sigma_j^2} \right] \exp \left[-\frac{\|i_p - \bar{n}_q\|^2}{\sigma_j^2} \right] \quad (3)$$

Where low-pass guidance is denoted as, i . Therefore, the filtering output $f(A)$ of the GABF is computed in Eq. (4):

$$f(A) = \sum_q X_{p,q}^{nuvf}(i, \bar{n}) i_q \quad (4)$$

An LPG image for a Gaussian range kernel is created as the first step in the suggested technique. A Gaussian kernel follows the noise filter's input. Edge-preserving image smoothing is possible using noiseless GABK.

3.3 Segmentation via attention V-net

In this section, the proposed method utilizes Attention V-net to segment the affected region of the fruit's images based on field observation. The digital data from the environmental field are also used to detect the occurrence of tea diseases for further segmentation. The backbone of the proposed segmented model is a V-net encoder-decoder structure. Feature extraction is performed by the encoder part, and resolution is restored by the decoder part. V-Net features are extracted using horizontal connections from the encoder to the decoder. A 3D attention gate can be worked as a connection component so that significant structural associations can be produced based on regional weight information paired with feature maps. This network is composed of four encoder blocks and four decoder blocks connected symmetrically by skip connections between the encoder and decoder. The

convolutional network is generally split up into stages in which each stage consists of one to three convolutional layers. Transposed convolution is also used in place of pooling in the upper and lower sampling sections. Furthermore, a structure is provided for the inclusion of residual connections at each level. SoftMax is used to transform the final convolution layer into a probabilistic foreground and background region segmentation.

During the image segmentation task, all hidden states play a significant role, but they are not equally significant. Convolution and pooling operations deepen the network through the V-Net. Ultimately, there will be more semantic information in the divided pixels in high-dimensional space. The contextual information from neighboring layers must be combined by a module, and the network must be guided by this information to identify the feature map's regions of interest. Therefore, self-attention is required to dynamically modify the significance of hidden values. In Squeeze Excitation's attention technique, the channels are multiplied by the coefficient of weight. Every value of each channel in the feature map has a distinct adjustment factor according to the proposed technique. Moreover, the feature maps and spatial weight information may be combined via the developed attention gate to improve semantic information and lower noise.

3.4 Sooty tern

The STO method is based on the natural behavior and lives of seabirds and is used as a clustering technique to locate user groupings. The STO algorithm finds relevant communities based on the similarity metric. The transition operation and the attack operation are the two primary phases in the STO algorithm. Terns migrate in large groups. Scarlet terns choose separate starting locations to prevent clashes. Sooty terns can travel the same distance as humans despite their poor fitness levels. Fig. 2 represents Flowchart of STO algorithm.

Migrating Behavior:

In this phase, the obtained best solution from aquila optimization is further optimized using STO for creating the cluster. The sooty tern follows the three criteria to migrate successfully:

Collision avoidance:

The position of the search agent (SA) is computed to prevent conflict with nearby search agents (e.g., sooty terns).

$$a_{ij} = N_{ik} \times m_{ij}(p) \quad (5)$$

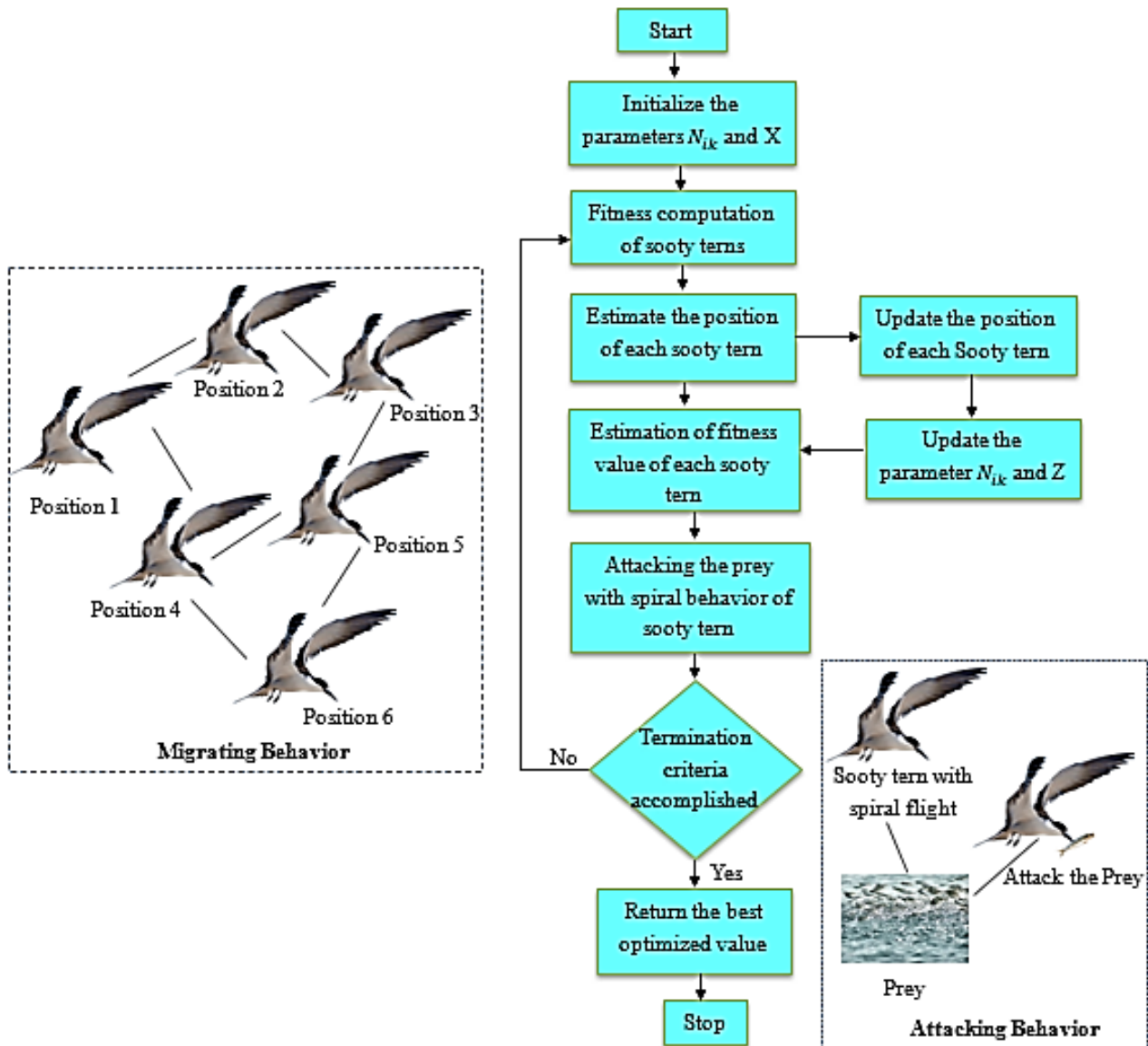


Figure. 2 Flowchart of STO algorithm

Converge in the direction of best neighbor: The search agents move in the direction of their closest neighbor to prevent collisions.

$$b_{ij} = X * (Y_{best}(P) - m_{ij}(p)) \quad (6)$$

The greater exploration is represented by the random variable X. X is derived in Eq. (7):

$$X = 0.5 * R_{and} \quad (7)$$

Where R_{and} is a random number that lies between the ranges from [0, 1].

Update corresponding to best search agent: The STO framework has been updated with new tactics

based on quantum mechanics theories and trajectory analysis to improve performance. It uses stochastic simulation to identify the elements that guarantee convergence. Updates are carried out using the following equations, by the quantum algorithm:

$$C_{ij}^{u+1} = S_{ij}^u \pm \alpha |Kbest_j^u - Z_{ij}^u| \ln \frac{1}{x} \quad (8)$$

$$c_{ij}^{u+1} = \begin{cases} S_{ij}^u \pm \alpha |Kbest_j^u - Z_{ij}^u| \ln \frac{1}{x}, & \text{if } m \text{ and } (0,1) \geq 0.5 \\ S_{ij}^u \pm \alpha |Kbest_j^u - Z_{ij}^u| \ln \frac{1}{x}, & \text{otherwise} \end{cases} \quad (9)$$

$$C_{ij} = \rho C_{ij} + (1 - \rho) C_{tj} \quad (10)$$

where C_{ij} denotes the gap between the search agent and the fittest search agent with maximum fitness value.

Attacking Behaviour:

In this phase, the selected best fitness users are clustered based on the similarity measure. During migration, these birds' wings assist them in reaching greater altitudes. The behavior is mathematically derived as,

$$l = S_{radius} \times \sin(i) \tag{11}$$

$$m = S_{radius} \times \cos(i) \tag{12}$$

$$n = S_{radius} \times j \tag{13}$$

$$D = a \times e^{kb} \tag{14}$$

where S_{radius} stands for the radius of each spiral round, i indicates that the variable within an interval of $\{0 \leq k \leq 2\pi\}$.

$$V_{ij}(p) = (C_{ij} \times (l + m + n)) \times Y_{best}(P) \tag{15}$$

where $V_{ij}(p)$ updates the positions of other SA and returns the best solution with clusters. The FC layer groups the pertinent user based on the output of the preceding layer using a few STO algorithmic clusters.

Algorithm: Sooty tern optimization

Input: population of users in social network

Output: Best cluster with best user Y_{best}

Procedure STO

Initialize the all the attributes

Calculate the fitness of each user using Eq. (4)

Update best user Optimal solutions can be achieved if they are better than the previous solution

Calculate the fitness of each cluster with the user

```

 $Y_{best} \leftarrow$  the best cluster with user
For each cluster with a user do
    Update the positions of the cluster with the
    user by using quantum theory Eqs. (8)-(10)
End for
Update the attributes SA and X
Calculate the fitness value of the cluster with
the user
Update  $Y_{best}$  If there is a better solution than
the previous optimal solution
return  $Y_{best}$ 
end procedure
    
```

3.5 Classification via GhostNet

In this module, ghost convolution uses only a portion of the feature map to avoid the feature map redundancy, created by standard convolution. The typical convolution simulation effect is then achieved in this section of the feature map by applying a straightforward linear transformation. Fig. 3 represents the Architecture of Ghost Network.

The $X \in R^{c \times h \times w}$ denotes the input feature map, c to denote the input feature map's channel count, and h and w to denote the feature map's height and breadth, respectively. The working of the conventional convolution is described in Eq. (16),

$$Y = X * f + b \tag{16}$$

A feature map with an output channel is represented by X in the equation above along with its height and width, which are denoted by h' and w' , respectively. The regular convolution after ignoring the error term is roughly identical to $h \times w \times c \times n \times w' \times h'$, which denotes the convolution operation, $k \times k$ is the size of the convolution kernel, and b is the error term.

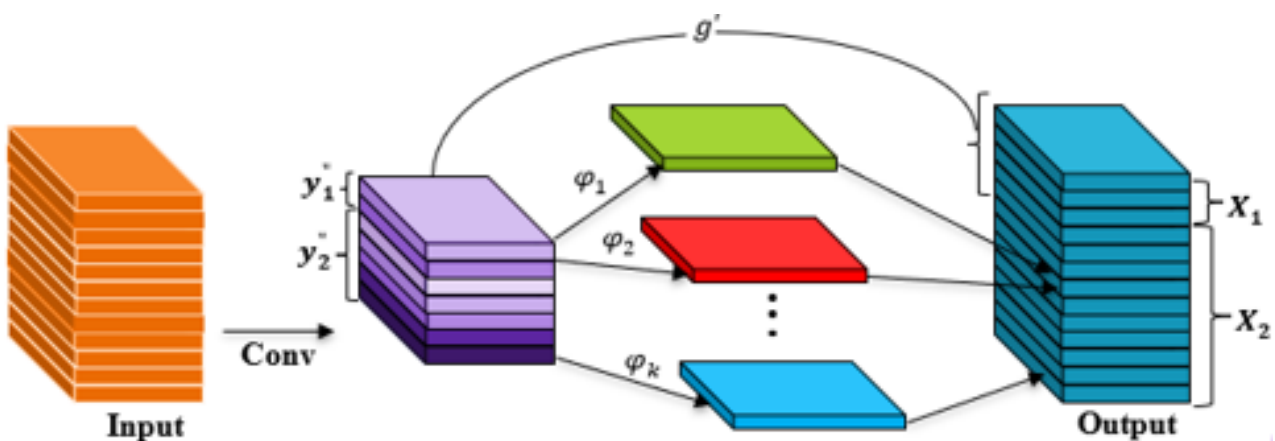


Figure. 3 Architecture of Ghost Network

h' and w' are larger in the shallow layer than n and c are in the deeper layer. Based on these characteristics, the concept of "ghost convolution," consists of two components: The light linear transform layer's redundant feature map is produced by the normal convolution kernel, which also produces a small number of feature maps. The following equation is described in Eq. (17).

$$Y' = X * f' + b \quad (17)$$

The output feature is represented by $Y' \in R^{h' \times w' \times m}$, and the size of this convolutional layer is represented by $f' \in R^{c \times k \times k \times m}$. This convolution layer generates a limited number of feature maps, the layer of convolution, and the multiplier for convolution. The output feature map has fewer channels, namely m , than a typical convolutional layer.

$$y_{ij} = \phi_{i,j}(y'_i) \quad (18)$$

In Eq. (5), where y_i stands for m feature maps of Y' , indicates the linear transform class that represents the creation of redundant feature maps. To produce s feature maps, each feature map in Y' goes through a small linear transformation called $\phi_{i,j}$ ($j = 1, 2, \dots, s$). If the $d \times d$ convolution is employed as the linear transform, the resulting linear transform must be constant. As a result, after linear transformations of $m \times (s - 1)$ feature maps, m feature maps are obtained. The result of applying Ghost convolution is $(s - 1) \times m \times h' \times w' \times k \times k$. The detection module uses a bounding box to find persons.

4. Result and discussion

The performance of the existing methods was compared with the performance of the proposed strategy to illustrate that it is more effective. In a comparative study, the SOOTY FRUIT is compared with three existing methods. SOOTY FRUIT proposed model is compared to DL methods like. Performance evaluation was based on various metrics such accuracy of the DL technique. The proposed technique is implemented using MATLAB2020b running on a Windows 10 OS with an Intel i3 core processor at 2.10 GHz and 8GB RAM.

4.1 Calorie estimation

The volume of the meal and an estimate of the caloric content are utilized to calculate the CV. CV are frequently utilized to quantify the entire amount of energy in each item, which includes the three

Table 1. Common calories table

Fruit Name	Measure	Weight in grams	Energy
Orange	1	140	64
Apple	1	150	50
Banana	1	101	10
Pears	1	178	100
Guava	1	100	285 kJ (68 kcal)

major nutritional constituents, carbs, protein, and fat.

The table includes an example of a calorie Table. 1. Every day, a particular number of CV must be consumed. Obesity can result from eating too many calories each day. Column one represents the Fruit name and two represents the Measure and Column three represents the weight in grams and Column four represents the energy. The volume of the meal and an estimate of the caloric content are utilized to calculate the CV. CV are frequently utilized to quantify the entire amount of energy in each item, which includes the three major nutritional constituents, carbs, protein, and fat. Experimental results of the proposed SOOTY FRUIT shown in Fig 4.

Column one represents the input image, Column two represents the pre-processed image, Column three represents the segmented image and Column four represents the Classified results with calories value.

In Fig. 5, the performance curve is illustrated by a vertical axis is illustrated as the accuracy range and a horizontal axis illustrates the number of epochs. As the number of epochs increases, the performance of the proposed increases.

According to Fig. 6, the loss of the SOOTY FRUIT diminishes as the epochs are raised. The proposed SOOTY FRUIT obtains high accuracy for inpainting the video caption gaps using the dataset. This analysis defined the number of training epochs required to achieve a high level of testing accuracy.

Fig. 7 demonstrates the performance of the SOOTY FRUIT approach better than the other methods. The accuracy of the SOOTY FRUIT technique can be as high as 99.95%, while that of traditional models like the CAE-AND, F-RCNN, and AFN is 84.9%, 87.58%, and 93.91%, respectively. The accuracy of the SOOTY FRUIT approach improved by 16.09%, 13.8%, and 3.75% when

compared to the existing methods, respectively. The SOOTY FRUIT strategy performs resiliently 16.58%, 13.29%, and 10.02% better than the existing methods.

The greatest F measurement of the SOOTY FRUIT approach is 99.11%, which is relatively high when compared to existing methods.



























Input Image	Pre-processed Image	Segmented Image	Classified result with calorie value
			 Calorie Value: 47  Calorie Value: 47  Calorie Value: 52  Calorie Value: 52  Calorie Value: 89  Calorie Value: 89
			 Calorie Value: 47  Calorie Value: 47  Calorie Value: 57
			 Calorie Value: 52  Calorie Value: 52
			 Calorie Value: 68  Calorie Value: 68  Calorie Value: 68

Figure. 4 Experimental results of the proposed

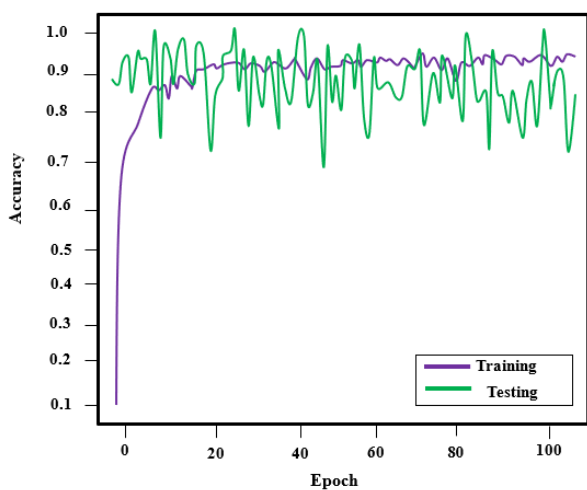


Figure. 5 Accuracy Curve for the proposed model

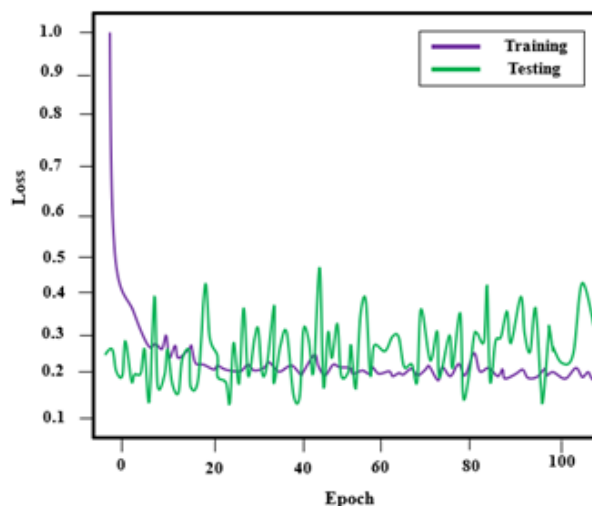


Figure. 6 Loss Curve for the proposed model

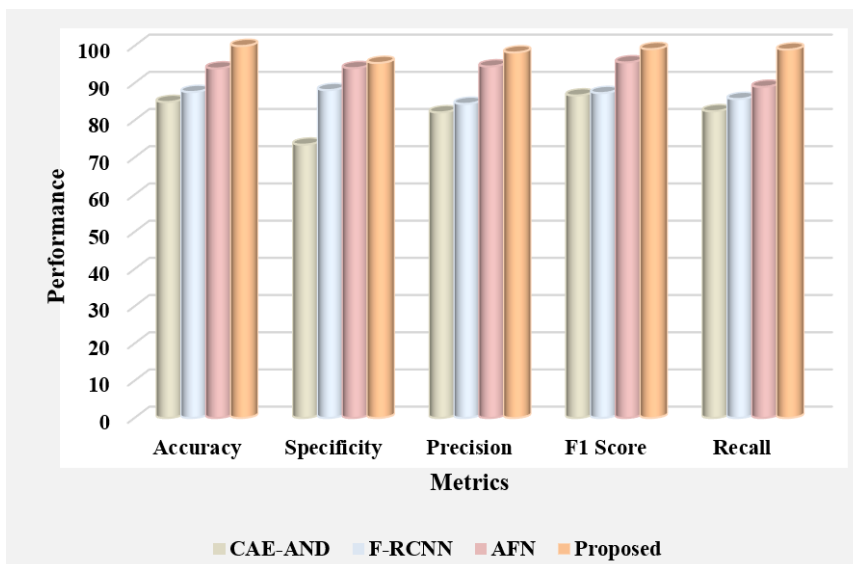


Figure. 7 Performance of the proposed with existing method

4.2 Discussion

In this section, a novel DL-based Fruits items classification method (SOOTY FRUIT) was proposed to classify different Fruits from the dataset by CV. The result section evaluates and analyses the proposed SOOTY FRUIT method's performance. The table includes an example of a calorie table. 1. Every day, a particular number of CV must be consumed. Obesity can result from eating too many calories each day. As compared to existing methods, the proposed SOOTY FRUIT shows better results in terms of Accuracy. The accuracy of the proposed technique can be as high as 99.95%, while that of traditional models like the CAE-AND, F-RCNN, and AFN is 84.9%, 87.58%, and 93.91%, respectively.

5. Conclusion

In this paper proposed a novel Deep Learning-based Fruits Items Classification (SOOTY FRUIT) method to classify the variety of Fruits items from the dataset with their calorie values (CV). In the first, the sigmoid stretching methods the images are processed utilized to increase the image quality and remove the noises. Consequently, the segmented images are pre-processed utilizing U-net algorithm. The extracted features are then normalized utilized the Sooty Tern Optimization Algorithm (STOA). Fruits items are classified using Ghostnet based on these relevant features. As compared to existing methods, the proposed SOOTY FRUIT shows better results in terms of Accuracy. The accuracy of the proposed technique can be as high as 99.95%, while that of traditional models like the CAE-AND, F-RCNN, and AFN is 84.9%, 87.58%, and 93.91%, respectively. The Proposed approach enhance the overall accuracy

of the suggested approach might overcome these difficulties in the future by utilizing hybrid DL techniques.

Conflicts of Interest

The authors declare that they have no known competing financial interests or personal relationships that could have appeared to influence the work reported in this paper.

Author Contributions

The following statements should be used as follows: Conceptualization, Josephin Shermila. P and Seethalakshmi. V; methodology, Ahilan. A; software, Devaki. M; validation, Josephin Shermila. P, Seethalakshmi. V, and Ahilan. A; formal analysis, Devaki. M; investigation, Josephin Shermila. P; resources, Seethalakshmi. V; data curation, Ahilan. A; writing—original draft preparation, Devaki. M; writing—review and editing, Josephin Shermila. P; visualization, Seethalakshmi. V; supervision, Ahilan. A; project administration, Devaki. M; funding acquisition, Josephin Shermila. P.

Acknowledgments

The author would like to express his heartfelt gratitude to the supervisor for his guidance and unwavering support during this research for his guidance and support.

References

- [1] F.A. Ogbale, and E.E. Sanugba, "Distribution of body mass index and abdominal obesity in Bayelsa State with associated interleukin-2 gene

- expression”, *Asian Journal of Biochemistry, Genetics and Molecular Biology*, Vol. 14, No. 4, pp.1-10, 2023.
- [2] S. Popat, and D. Shabiethaa, “Levels of Physical Activity and Prevalence of Obesity among Undergraduate Physiotherapy Students in Navi Mumbai: A Descriptive Study”, *EDITORIAL BOARD*, Vol. 17, No. 1, pp. 100, 2023.
- [3] A.K. Jawad, and A.A. Okab, “Prevalence of Obesity and Overweight among Staff at Technical Institute-Swaira in Middle Technical University”, *Diyala Journal of Medicine*, Vol. 24, No. 1, pp.225-234, 2023.
- [4] S. Chilufya, Prevalence of Overweight and Obesity and its Associated Factors among Medical Students: A Case of Copperbelt University School of Medicine, Ndola, Zambia. *Global Journal of Health Sciences*, Vol. 8, No. 1, pp. 72-96, 2023.
- [5] M.A. Zemene, D.T. Anley, N.A. Gebeyehu, Adella, G.A., Kassie, G.A., Mengstie, M.A., Seid, M.A., Abebe, E.C., Gesese, M.M., Tesfa, N.A. and Y.S. Kebede, “Concurrent stunting and overweight or obesity among under-five children in sub-Saharan Africa: a multilevel analysis”, *Archives of Public Health*, Vol. 81, No. 1, pp. 119, 2023.
- [6] J.M. Were, S. Stranges, and I.F., Creed, “Fertility is a key predictor of the double burden of malnutrition among women of child-bearing age in sub-Saharan Africa”, *Journal of global health*, Vol. 10, No. 2, 2020.
- [7] N.P. Steyn, and J.H. Nel, “Prevalence and Determinants of the Double Burden of Malnutrition with a Focus on Concurrent Stunting and Overweight/Obesity in Children and Adolescents”, *Current Nutrition Reports*, Vol. 11, No. 3, pp.437-456, 2022.
- [8] T. Reardon, D. Tschirley, L.S.O. Liverpool-Tasie, T. Awokuse, J. Fanzo, B. Minten, R. Vos, M. Dolislager, C. Sauer, R. Dhar, and C. Vargas, “The processed food revolution in African food systems and the double burden of malnutrition”, *Global food security*, Vol. 28, pp. 100466, 2021.
- [9] A.Z. Alem, Y. Yeshaw, A.M. Liyew, Z.T. Tessema, M.G. Worku, G.A. Tesema, T.S. Alamneh, A.B. Teshale, D. Chilot, and H.G. Ayalew, “Double burden of malnutrition and its associated factors among women in low and middle income countries: findings from 52 nationally representative data”, *BMC Public Health*, Vol. 23, No. 1, pp.1479, 2023.
- [10] Ž. Ahčin, J. Liang, K. Engelbrecht, and J. Tušek, “Thermo-hydraulic evaluation of oscillating-flow shell-and-tube-like regenerators for (elasto) caloric cooling”, *Applied Thermal Engineering*, Vol. 190, pp. 116842, 2021.
- [11] L. Alexander, S.M. Christensen, L. Richardson, A.B. Ingersoll, K. Burrige, A. Golden, S. Karjoo, D. Cortez, M. Shelver, and H.E. Bays, “Nutrition and physical activity: an obesity medicine association (OMA) clinical practice statement 2022”, *Obesity Pillars*, Vol. 1, pp. 100005, 2022.
- [12] H.E. Bays, A. Golden, and J. Tondt, “Thirty obesity myths, misunderstandings, and/or oversimplifications: an obesity medicine association (OMA) clinical practice statement (CPS) 2022”, *Obesity Pillars*, Vol. 3, pp. 100034, 2022.
- [13] G. Xue, S. Liu, and Y. Ma, “A hybrid deep learning-based fruit classification using attention model and convolution autoencoder”, *Complex & Intelligent Systems*, pp. 1-11, 2020.
- [14] S. M. Wasif, S. Thakery, A. Nagauri, S. I. Pereira, “Food calorie estimation using machine learning and image processing”, *International Journal of Advance Research, Ideas and Innovations in Technology*, Vol. 5, pp. 1627-1630, 2019.
- [15] H. S. Gill, O. I. Khalaf, Y. Alotaibi, S. Alghamdi, and F. Alassery, “Fruit image classification using deep learning”, *Computers, Materials & Continua*, 2022, doi: 10.32604/cmc.2022.022809.
- [16] H. Mahgoub, G. Aldehim, N.S. Almalki, I. Issaoui, A. Mahmud, and A.A. Alneil, “Bio-Inspired Spotted Hyena Optimizer with Deep Convolutional Neural Network-Based Automated Food Image Classification”, *Biomimetics*, Vol. 8, No. 6, pp.493, 2023.
- [17] Y. Gulzar, “Fruit image classification model based on MobileNetV2 with deep transfer learning technique”, *Sustainability*, Vol. 15, No. 3, pp.1906, 2023.
- [18] Y.D. Zhang, Z. Dong, X. Chen, W. Jia, S. Du, K. Muhammad, and S.H. Wang, “Image based fruit category classification by 13-layer deep convolutional neural network and data augmentation”, *Multimedia Tools and Applications*, Vol. 78, pp.3613-3632, 2019.
- [19] C. Liu, Y. Liang, Y. Xue, X. Qian, and J. Fu, “Food and ingredient joint learning for fine-grained recognition”, *IEEE Transactions on Circuits and Systems for Video Technology*, Vol. 31, No. 6, pp.2480-2493, 2020.
- [20] Z. Wang, W. Min, Z. Li, L. Kang, X. Wei, X. Wei, and S. Jiang, “Ingredient-Guided Region Discovery and Relationship Modeling for Food Category-Ingredient Prediction”, *IEEE Transactions on Image Processing*, Vol. 31, pp. 5214-5226, 2022.